Engineering Science and Technology, an International Journal 21 (2018) 704–713

HOSTED BY

Contents lists available at ScienceDirect

Engineering Science and Technology, an International Journal

journal homepage: www.elsevier.com/locate/jestch

Full Length Article

A new electric braking system with energy regeneration for a BLDC motor driven electric vehicle

A. Joseph Godfrey *, V. Sankaranarayanan

Control Systems Research Laboratory, Department of Electrical and Electronics Engineering, National Institute of Technology-Tiruchirappalli, Tiruchirappalli 620015, Tamilnadu, India

ARTICLE INFO

Article history:
Received 15 December 2017
Revised 1 April 2018
Accepted 5 May 2018
Available online 24 May 2018

Keywords:
BLDC motor
Electric vehicle
Electric braking
Regenerative braking
Braking strategy

ABSTRACT

A new electric braking system is proposed for a brushless DC (BLDC) motor driven electric vehicle (EV) in this paper based on stopping time and energy regeneration. This new braking system is developed by combining various regenerative methods and plugging. Other than the existing performance measures such as boost ratio, braking torque, and maximum conversion ratio; stopping time and energy recovery for various methods are studied for different running conditions. It is observed that the stopping time is less for plugging and increases in the order of two, three and single switch method. In addition, energy recovery is better for single and three switch method. Based on these performances, a new braking strategy is proposed which combine all the regenerative braking methods including plugging and switch among themselves based on the brake pedal depression. The effectiveness of the proposed method is shown using both simulation and experiment results.

1. Introduction

Electric vehicle (EV) is one of the alternatives to internal combustion engine powered vehicle due to pollution concern, cost and availability of the oil. These vehicles are propelled by electric motors of either AC or DC. DC motors are mainly used for propulsion since batteries are used as the main power source. In recent days, due to the advancement in power electronic converters, motors such as brushless DC (BLDC) motors, permanent magnet synchronous motors (PMSM) and switched reluctance motors are used [1,2]. Among these, BLDC motors are often used due to high efficiency, high power density, large starting torque, noiseless operation, low weight and smaller in size [3]. Recent vehicles are powered by hub type BLDC motors, motors in-build in the wheel, to avoid complex power train mechanism [4].

Range (driving range) of the EV, the distance traveled by the vehicle per charge, is an important parameter. Improving the range is the main objective for most of the EV manufacturer. The range can be improved by increasing the efficiency of the overall components including the motor, power converter, and battery. Regenerative braking is one of the methods to increase the range by charging the battery from the energy available during braking. During regenerative braking, the vehicle inertia together with power electronic converters makes the motor to act as the generator to send the energy back to the battery [5,6]. Studies are ensuring that the driving range can be improved by 8–25% using regenerative braking [7].

Regenerative braking is achieved through various methods in EVs. In [8–11], regenerative braking is achieved using additional DC-DC converter which boosts the back electromotive force (back-EMF) to the appropriate level to charge the battery. This method requires extra converter which increases the cost and weight of the system. In [12–15], regenerative braking is achieved using ultracapacitor connected either in series or parallel with batteries. The ultracapacitor stores the regenerative energy surge and sends it back to the battery with the help of additional converters. This method also increases the cost and weight of the overall system.

Regenerative braking is achieved using electronic gear shift technology [16,17] in which the electronic gear forms different serial and parallel connections of batteries, motor winding, and ultracapacitor based on vehicle speed to recover regenerative energy. This method requires specially designed motors with multiple windings, various battery connections, and multiple switches. Moreover, a complex switching topology has to be developed for implementation.

To overcome the disadvantages of various regenerative scheme discussed [8–17], an alternative method is proposed using the single stage converter which drives the BLDC motor. The single stage converter is able to perform regenerative braking by applying

* Corresponding author.
E-mail address: josephgdfry@gmail.com (A. Joseph Godfrey).
Peer review under responsibility of Karabuk University.

https://doi.org/10.1016/j.jestch.2018.05.003
2215-0986/

switching pulses in a proper sequence without any additional power converter. In this single stage converter, different types of braking methods based on different switching topology namely single switch, two switch and three switch are studied [18,19]. Based on the study, it is concluded that single switch and three switch are capable of producing required braking torque and better energy recovery in mid to high-speed range. Moreover, two switch is recommended for low speed or emergency braking case since it produces high braking torque. Regenerative braking using the single switch and two switch are also studied in [15,20–22]. Recently a fully electrical regenerative braking is proposed for very fast and precise braking torque control [23]. However, use of regenerative braking alone is not effective at low speeds and for emergency case [24,25].

In order to ensure effective braking at all speeds, this paper proposes a new electrical braking system for a BLDC driven EV based on various electric braking methods such as single, two, three switching topologies and plugging. The performance indices such as boost ratio, braking torque, and maximum voltage conversion ratio are studied for each braking method. In addition, stopping time and energy recovery are studied through simulation and experiment for different running conditions. Based on stopping time and energy recovery, a new braking strategy is developed to combine different regenerative method and plugging using brake pedal depression.

The paper is organized as follows. Section 2 describes the conventional electric braking methods and stopping time. In Section 3, the performance of the braking methods is studied by simulation and experimentation. Section 4 explains the implementation of a proposed braking system based on brake pedal depression and followed by the conclusion in Section 5.

2. Conventional electric braking methods and stopping time

2.1. Single stage electric braking methods

In single stage electric braking method, the braking and energy regeneration are achieved by the use of single stage bidirectional DC/AC converter which is used to drive the BLDC motor. The BLDC motor driven by a single stage bidirectional converter is shown in Fig. 1. R and L are the phase resistance and phase inductance respectively. E_a, E_b, E_c and I_a, I_b, I_c are back-EMF and armature currents respectively. S_1 *to* S_6 are switches and D_1 *to* D_6 are the freewheeling diodes and C is the DC link capacitor. A dedicated controller is used to switch the inverter in a particular fashion based on the rotor position received from hall sensors H_a, H_b and H_c. The switching sequences and the switches incorporated in achieving various braking methods such as single switch, two switch, three switch, and plugging are shown in Fig. 2. The performance parameters are given in Table 1.

In single switch braking method, only one switch out of switches S2, S4, S6 is operated in pulse width modulation (PWM) switching mode at each commutation state [15,20]. In two switch method, two switches out of switches S1-S6 are operated in PWM switching mode at each commutation state [21,22]. In three switch method, three switches S2, S4, S6 are operated in PWM switching mode at the same time in each commutation state [18,19]. The switching sequence of plugging is similar to that of two switch method, where a continuous signal is applied instead of PWM pulses [26]. The performance indices of these braking methods such as boost ratio, braking torque and maximum voltage conversion ratio [18,19] are presented in Table 2.

2.2. Stopping time calculation

In addition to the performance indices [18,19], the stopping time of each braking method is obtained in this paper.

The motor dynamics can be expressed as

$$J\frac{d\omega}{dt} + B\omega + T_l = T_e \tag{1}$$

On neglecting the friction coefficient and load torque, Eq. (1) can be simplified as

$$J\frac{d\omega}{dt} = T_e \tag{2}$$

While braking, the motor torque T_e becomes negative and is written as $T_e = -K_t i_a$. Therefore

$$J\frac{d\omega}{dt} = -K_t i_a \tag{3}$$

The equation of braking current for the single switch method at steady state is [27],

$$i_a = \frac{D(2V_{emf})}{R_b + 2R} \tag{4}$$

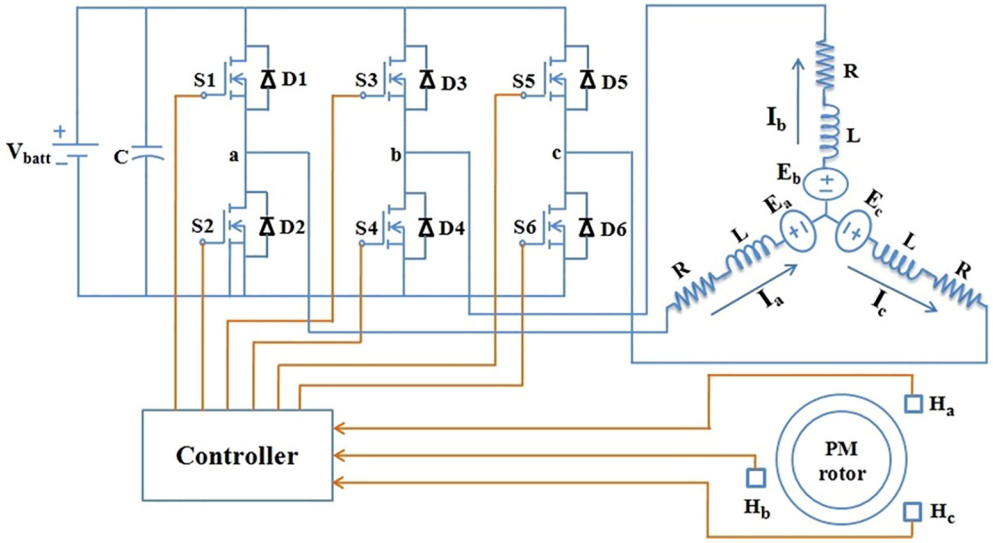

Fig. 1. Equivalent circuit of BLDC motor.

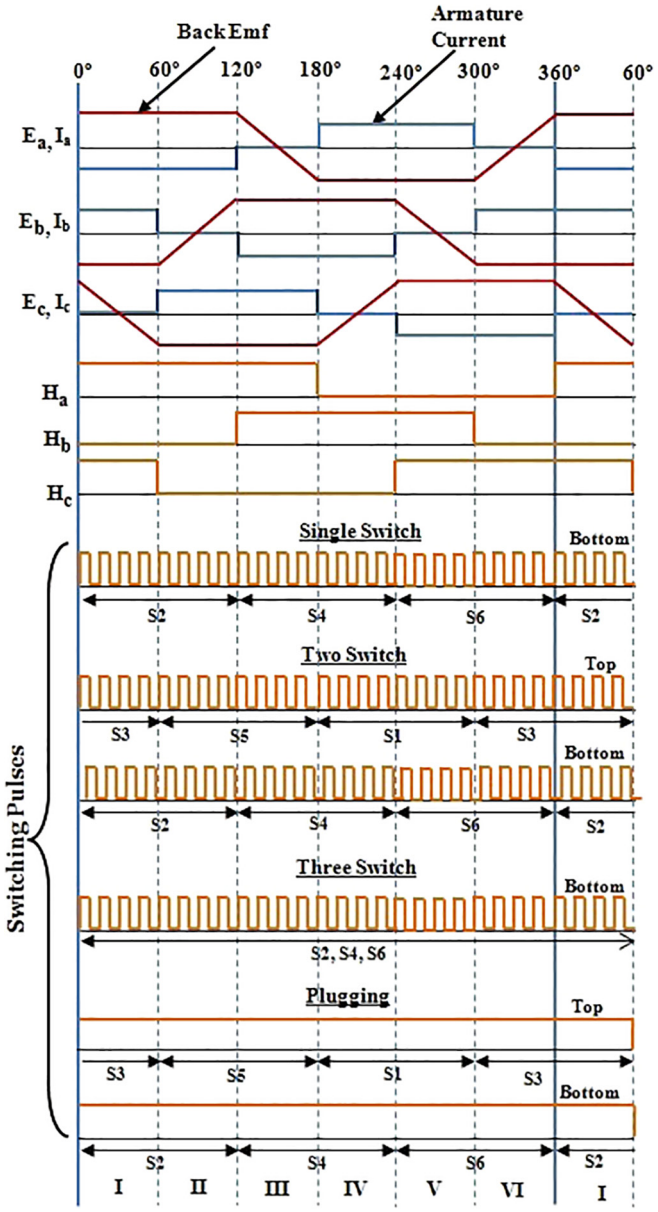

Fig. 2. Switching sequence of conventional electric braking methods.

Table 1
List of symbols.

Symbol	Description
V_{batt}	Battery voltage
$2V_{emf}$	Line back-EMF
R	Armature resistance per phase
R_b	Equivalent load resistance of battery comprising of internal resistance and the resistance due to chemical reaction
K	Ratio of R to R_b
D	Duty cycle
D'	$1 - D$
i_a	Armature current
T_{max}	Maximum voltage conversion ratio
J	Moment of inertia
B	Friction coefficient
ω	Angular velocity
T_l	Load torque
T_e	Motor torque
K_t	Motor torque constant

Table 2
Performance indices of conventional electric braking methods.

	Single switch	Two switch	Three switch	Plugging
Boost ratio	$\frac{2}{D'+\frac{2K}{D'}}$	$\frac{2}{(2D'-1)+\frac{2K}{(2D'-1)}}$	$\frac{2}{D'+(\frac{7}{4})(\frac{K}{D'})}$	–
Braking torque	$\frac{K_t(2V_{emf})}{D'^2R_b+2R}$	$\frac{K_t(2V_{emf})}{(2D'-1)^2R_b+2R}$	$\frac{K_t(2V_{emf})}{D'^2R_b+(\frac{7}{4})R}$	$\frac{K_t(2V_{emf})}{R_b+2R}$
$T_{max}(D')$	$\frac{1}{\sqrt{2K}}$	$\pm\frac{1}{\sqrt{2K}}$	$\frac{1}{\sqrt{\frac{7}{8}K}}$	–
Deceleration	$-\frac{K_tD(2V_{emf})}{J(R_b+2R)}$	$-\frac{K_t(2V_{emf}+DV_{batt})}{J(R_b+2R)}$	$-\frac{K_tD(2V_{emf})}{J(R_b+\frac{7}{4}R)}$	$-\frac{K_t(2V_{emf}+V_{batt})}{J(R_b+2R)}$

Table 3
Deceleration values of braking methods.

Braking Method	Deceleration (rad/sec^2)
Single	−38.43
Three	−39.14
Two	−158.84
Plugging	−240.82

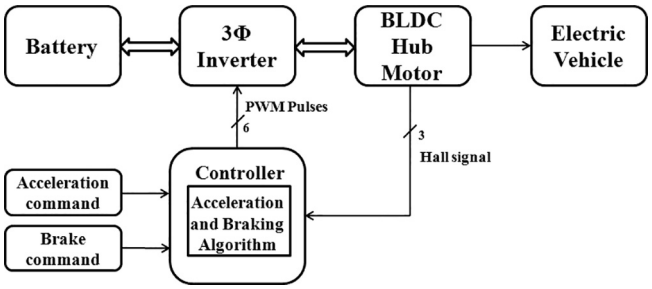

Fig. 3. Block diagram for performance evaluation of various electric braking methods.

Table 4
Specification of BLDC motor.

Parameters	Value
Number of phases	3
Stator phase resistance (ohm)	0.17
Stator phase inductance (H)	$256e^{-6}$
Flux linkage established by magnets (V.s)	0.023354
Voltage Constant ($V_{peak\ L\text{-}L}$/krpm)	112.5
Torque constant (N.m/A_{peak})	1.0743
Inertia J(kg.m^2)	0.1344
Viscous damping F(N.m.s)	0.084
Pole pairs	23
Static friction Tf(N.m)	0

By substituting (4) in (3) and rearranging, the deceleration of single switch is

$$\frac{d\omega}{dt} = -\frac{K_tD(2V_{emf})}{J(R_b+2R)} \tag{5}$$

Similarly the expression for two switch, three switch and plugging are derived and are tabulated in the Table 2. To highlight the distinction of deceleration among the braking methods, the amount of deceleration is calculated for motor running at a specific speed, fixed battery voltage and at a particular duty cycle. The motor parameters are as in Table 4, $R_b = 2\Omega$, $2V_{emf} = 22.5$ V (corresponds to 200 rpm), $V_{batt} = 48$ V and $D = 0.5$. The deceleration for single switch is

$$\frac{d\omega}{dt} = -\frac{1.0743 \times 0.5 \times 22.5}{0.1344 \times (2 + 2 \times 0.17)} = -38.43 \frac{rad}{sec^2} \quad (6)$$

Similarly, calculations are carried out for two switch, three switch and plugging and are presented in Table 3. It is noted that the deceleration of single switch is less and increases in the order of three, two and plugging. So the stopping time of the single switch is high and decreases in the order of three, two and plugging.

3. Performance evaluation

The performance of various braking methods is carried out using both simulation and experiments. Stopping time and average energy recovery are studied from the simulation results for various speed and state of charge (SOC) of the battery. The block diagram of the performance evaluation study is depicted in Fig. 3. The simulation model constitutes a battery, three phase inverter, BLDC motor and a control module. The control module is programmed with various braking methods such as plugging, single switch, two switch and three switch. The acceleration and brake commands are given to the control module that drives the motor for various driving conditions. When acceleration command is applied, the brake command is made inactive and vice versa. The parameter used for simulation is given in Table 4.

3.1. Simulation results

For the performance evaluation, first the BLDC motor is subjected to run at a constant speed to apply brake signal. Each braking methods are studied for various duty cycle while maintaining battery SOC constant.

3.1.1. Stopping time

Fig. 4 shows the comparison of stopping time among the braking methods at various speed and SOC level. For a particular motor speed and SOC level as shown in Fig. 4(a), the stopping time is less for plugging and increasing from two, three and single switch respectively. With the duty cycle increase, the stopping time of all the braking methods again decreases with a higher rate. The stopping time for plugging is constant since the duty cycle is constant. In Fig. 4(a) and (b), the stopping time is compared with a SOC level of 80% for the speed of 400 rpm and 200 rpm. In general, the stopping time of a motor depends upon the speed at which it is running. In Fig. 4a and (b), the stopping time of motor running at 200 rpm take less time to stop compared to the motor running at the speed at 400 rpm for all the methods and the same pattern is followed. Similarly in Fig. 4(c) and (d), the stopping time is compared with a SOC level of 50% for the speed of 400 rpm and 200 rpm and the same scenario can be observed.

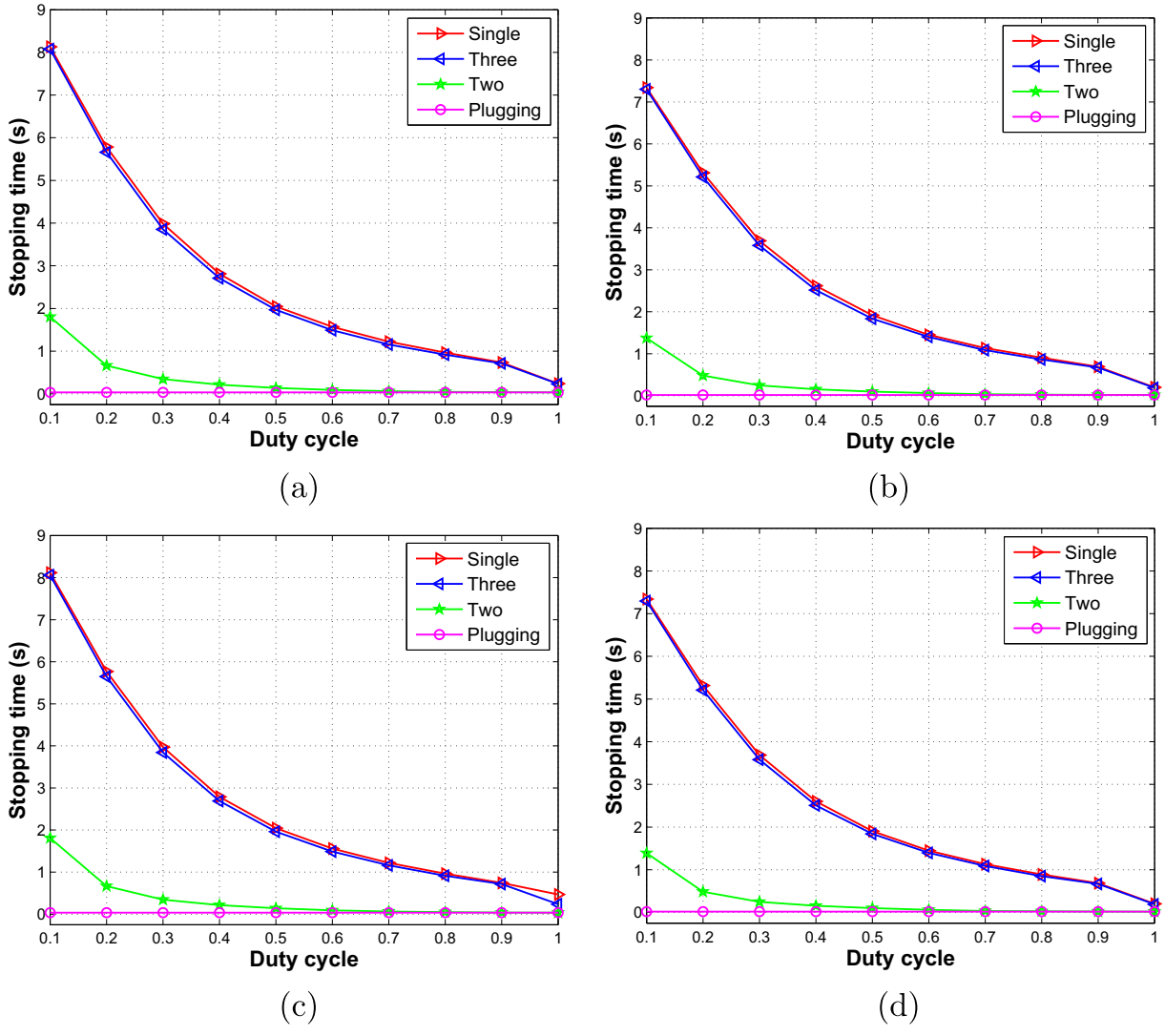

Fig. 4. Simulation results for stopping time versus duty cycle for various SOC and speed. (a) SOC = 80%, speed = 400 rpm. (b) SOC = 80%, speed = 200 rpm. (c) SOC = 50%, speed = 400 rpm. (d) SOC = 50%, speed = 200 rpm.

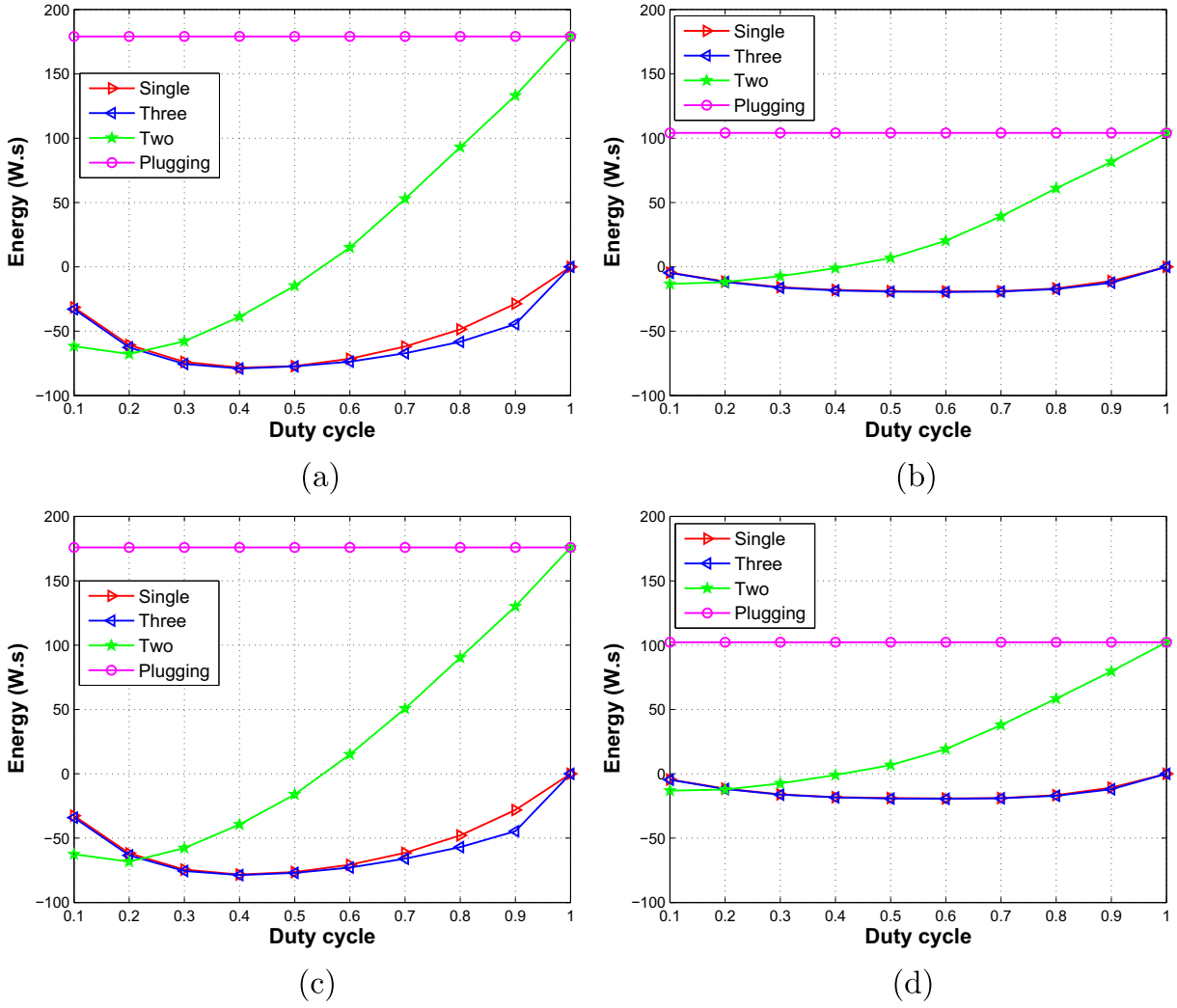

Fig. 5. Simulation results for average energy recovered versus duty cycle for various SOC and speed. (a) SOC = 80%, speed = 400 rpm. (b) SOC = 80%, speed = 200 rpm. (c) SOC = 50%, speed = 400 rpm. (d) SOC = 50%, speed = 200 rpm.

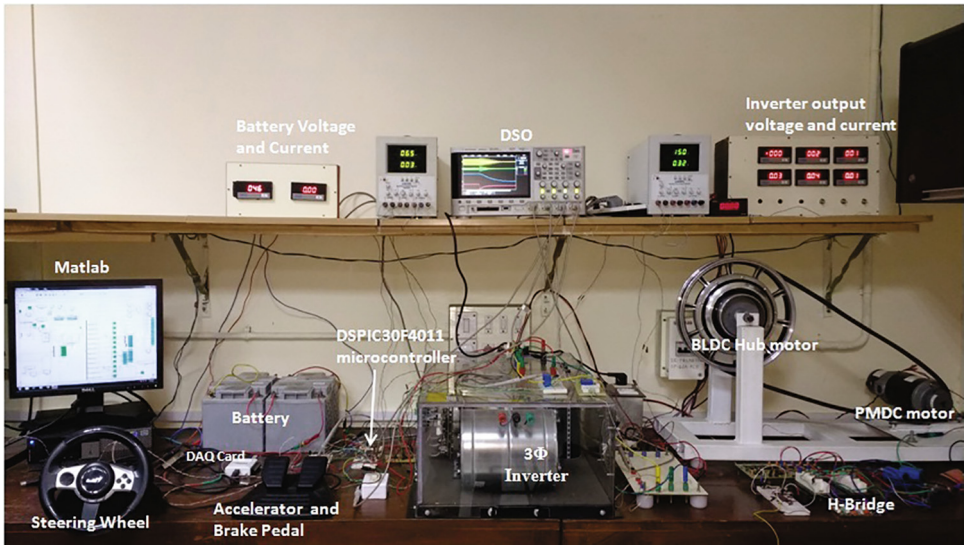

Fig. 6. Experimental setup.

3.1.2. Average energy recovered

The average energy recovered during the braking period is compared for various speed and SOC level in Fig. 5. The average energy is the area under the power versus time curve over the braking period. During a particular speed with a SOC level as shown in Fig. 5(a), the energy recovered by three switch is higher among all the braking methods. The energy recovered in the single switch is lesser than the three switch. As the duty cycle increases, the average energy recovered first increase to a peak value and then decreases and finally reaches zero when duty cycle attains one. In plugging, the energy is consumed rather than recovery during braking and it is positive. In two switch, as seen in Fig. 5(a), the average energy is negative during the duty cycle ranging from 0 to 0.5 and positive during 0.5 to 1. This is because that, during the duty cycle from 0 to 0.5, the amount of energy recovered is more compared to the amount of energy consumed from the battery over the braking period. Also when the duty cycle ranges from 0.5 to 1, the amount of energy recovered is less compared to the amount of energy consumed from the battery and it is positive. So in two switch, effective regeneration occurs in the duty cycle range from 0 to 0.5.

Now the average energy is compared to the motor running at a speed of 400 rpm and 200 rpm with 80% SOC level as shown in Fig. 5(a) and (b). From these figures, it is observed that the average energy recovered and average energy consumed for the speed 200 rpm is less in all the methods compared to the speed of 400 rpm. It can be clearly seen in Fig. 5(b) that the amount of energy consumed during plugging is less compared to the motor running at 400 rpm in Fig. 5(a). Similarly, the same comparison is done for the motor running at 400 rpm and 200 rpm with 50% SOC level as shown in Fig. 5(c) and (d) and the same scenario can be observed.

Table 5
Stopping time and average current for various duty cycle.

Duty cycle	Stop time (s)				Average current (A.s)			
	Single	Three	Two	Plugging	Single	Three	Two	Plugging
0.2	2.2	2.15	1.09	0.23	−0.112	−0.214	−0.189	0.942
0.4	1.49	1.39	0.5	0.23	−0.239	−0.247	−0.091	0.942
0.6	1.01	0.99	0.26	0.23	−0.286	−0.289	0.355	0.942
0.8	0.75	0.7	0.24	0.23	−0.234	−0.244	0.889	0.942

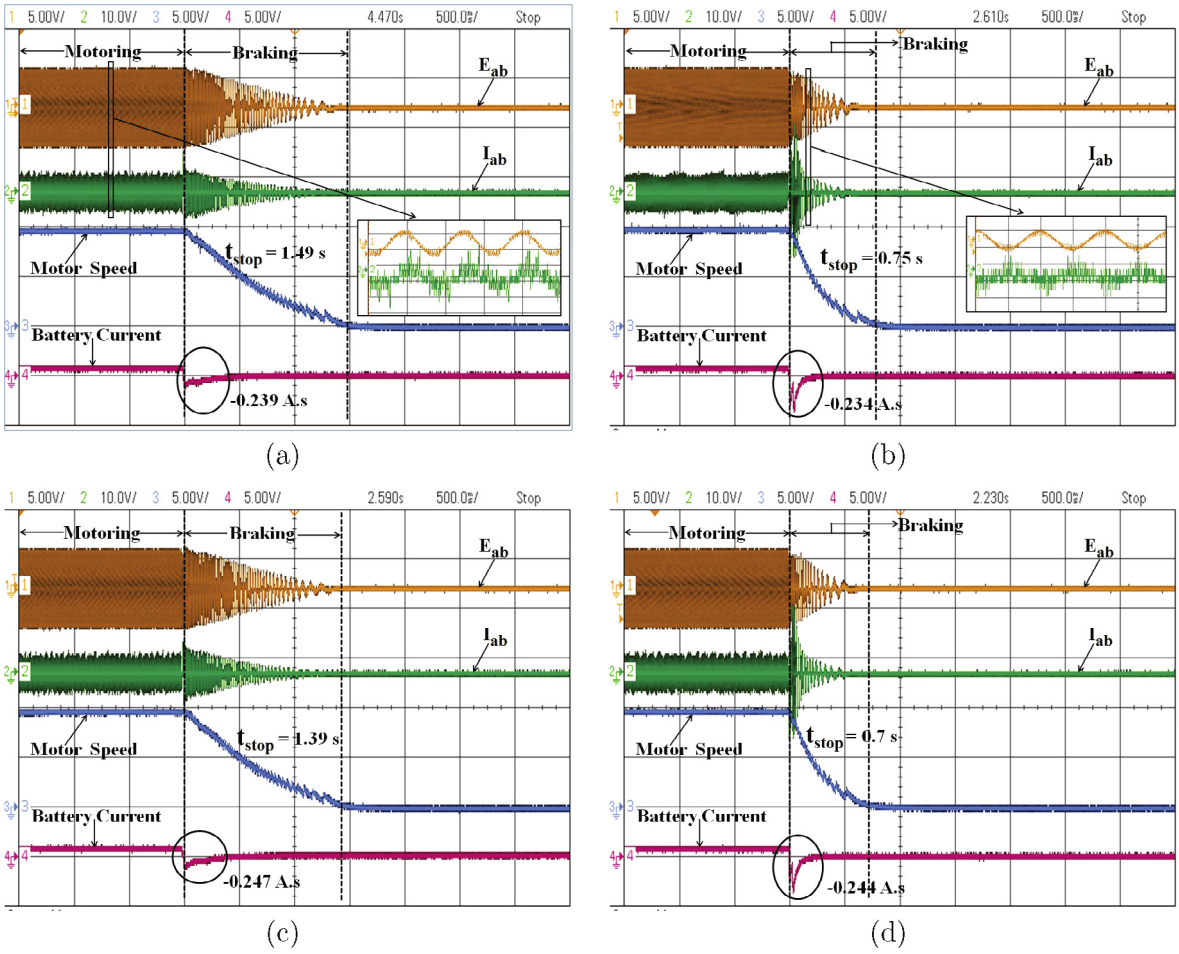

Fig. 7. Experiment results of performance evaluation for single switch and three switch for a specific SOC and speed. (a) single switch-0.4 duty cycle. (b) single switch-0.8 duty cycle. (c) three switch-0.4 duty cycle. (d) three switch-0.8 duty cycle.

3.2. Experimental procedure

In order to study the performance of different braking methods in real time, an experimental setup is built in the laboratory which emulates an EV. The experimental setup consists of a 48 V, 26 Ah battery, a three-phase inverter to drive the BLDC motor, digital controller, BLDC hub motor and permanent magnet DC (PMDC) motor for loading purpose. The specification of the BLDC motor is same as used for simulation, which is given in Table 4.

The digital controller dspic30f4011 is used as a PWM generator for the three-phase inverter to drive the BLDC motor. A PMDC motor is connected to the BLDC motor through a belt which acts as a load that mimics the effect of uphill and downhill driving conditions.

The performance study of each braking method is conducted separately for a specific level of SOC and speed with various duty cycle similar to simulation study. The variation of parameters such as back-EMF, armature current, stopping time and battery current is observed in the digital storage oscilloscope (DSO) from the point of braking to zero speed of the motor. The stopping time and average regenerative current over the braking period for various duty cycle are recorded and the summary is shown in the Table 5. The motor is accelerated to run at a speed of 340 rpm and subjected to braking after it attains steady speed. Figs. 7 and 8 show the waveforms of back-EMF, armature current, speed, and battery current in motoring region as well as braking regions for the duty cycle of 0.4 and 0.8 under 50% SOC level.

In the experimental results, it is observed that in the motoring region, the value of back-EMF is high corresponding to the steady speed and the armature current is in phase with the back-EMF. The battery current waveform in this region is positive. When subjected to braking, the back-EMF starts decreasing and finally reaches to zero. The armature current first increases and then decreases gradually and is in out of phase with the back-EMF. The zoomed view of back-EMF and armature current in motoring region and braking region are shown in Fig. 7(a) and (b) respectively. It is clearly observed that, in motoring region, back-EMF and armature current are in phase and in the braking region, the back-EMF and armature current is in out of phase. The battery current waveform changes from positive to negative representing the occurrence of regeneration and is indicated by circles.

The stopping time of each braking method is examined from the speed waveform. For the duty cycle of 0.4 as shown in Figs. 7 and 8, it can be seen that the stopping time is less for plugging and increasing from two, three and single switch. Again, for the duty cycle of 0.8, the same pattern is followed but the stopping time of all the methods is reduced. By this observation, it is confirmed that as the duty cycle increases the stopping time of each braking method decreases with the same pattern.

The battery current waveform is observed in the view of energy recovery as shown in Figs. 7 and 8. For the duty cycle of 0.4 and 0.8, it can be observed from Fig. 7 that, the average regenerated current in three switch is higher than the single switch. In two switch as shown in Fig. 8(a) and (b), regeneration occurs for 0.4 duty cycle

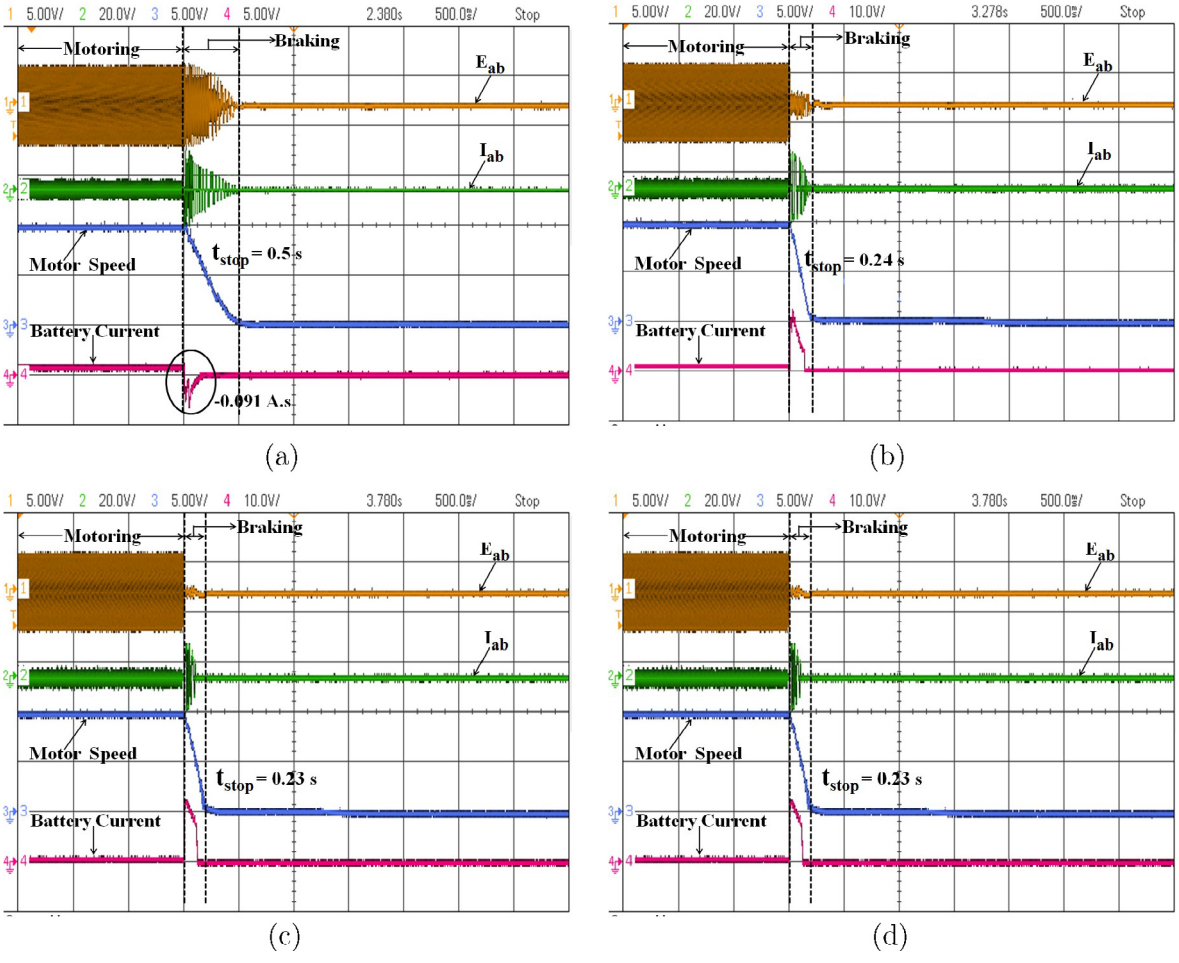

Fig. 8. Experiment results of performance evaluation for two switch and plugging for a specific SOC and speed. (a) two switch-0.4 duty cycle. (b) two switch-0.8 duty cycle. (c) plugging-0.4 duty cycle. (d) plugging-0.8 duty cycle.

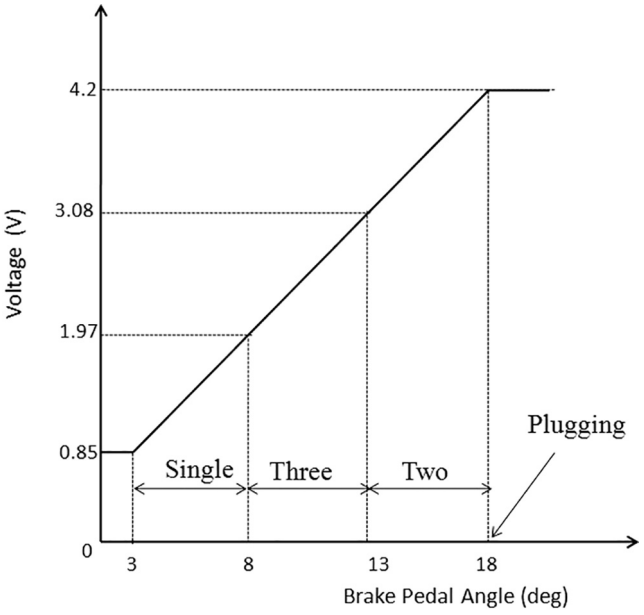

Fig. 9. Brake pedal angle vs output voltage.

Fig. 10. Picture of brake pedal.

and no regeneration occurs in 0.8 duty cycle. In plugging as shown in Fig. 8(c) and (d), it is clearly seen that more battery current is consumed for stopping the motor and no regeneration occurs.

4. Proposed braking system

Based on the results obtained from the performance evaluation of various braking methods, a new braking strategy is proposed based on stopping time(deceleration) and energy recovery. The strategy switches the braking methods in a sequence as shown in Fig. 9 based on the brake pedal depression.

The brake pedal employed here is a linear hall effect based pedal whose output voltage varies between 0.85 V and 4.2 V when depressed from 0° to 18°. The picture of the brake pedal used is shown in Fig. 10. A tolerance of 3° is given from the initial point of the brake pedal as a safety measure and no braking method is alloted. When the pedal is depressed above 3°, the single switch is activated and again when depressed above 8°, three switch is activated. Above 13°, two switch is activated and at 18°, plugging is activated. As single switch and three switch has less deceleration and more energy recovery, it is adapted for normal braking event or deceleration purpose. Hence, these methods are placed at the initial angle (3°–13°) of the brake pedal. As the deceleration of two switch and plugging is high, two switch is adapted for rapid stopping condition and plugging for emergency cases. So these methods are placed at the final angle (13°–18°) of the brake pedal.

4.1. Simulation and experimental results

The working of proposed braking strategy is verified using both simulation and experimental results. Simulation is performed in the simulation model considered in performance evaluation. The brake pedal for the simulation is realized by ramp signal with various slopes and different voltage levels. Experimental test is conducted in the experimental setup shown in Fig. 6. Both the tests are carried out by accelerating the motor to run at a speed of 412 rpm with 80% SOC level. The tests are conducted in a sequence as explained as follows. After the motor reaches the steady speed, initially brake pedal is depressed slightly to a level to activate single switch method. The motor stops and after some time, the motor

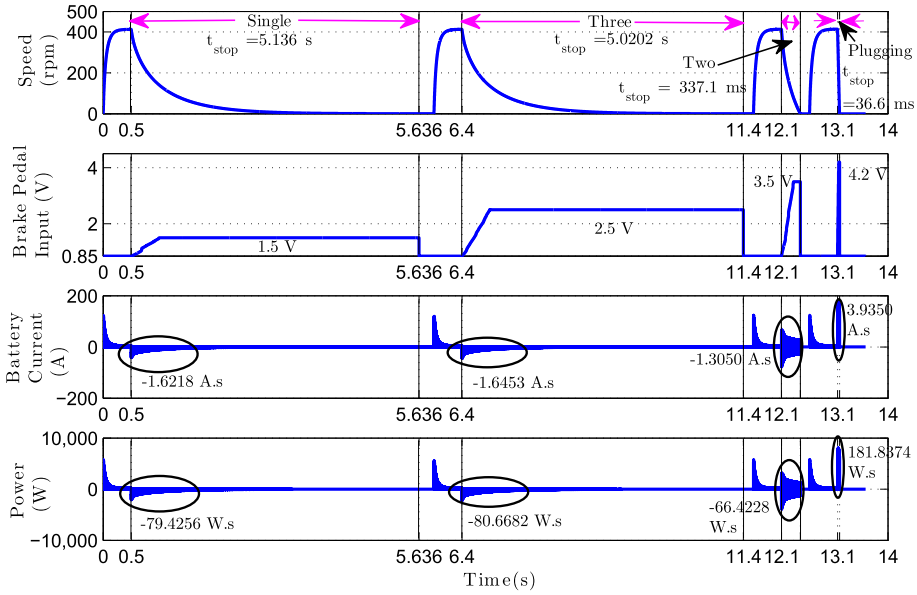

Fig. 11. Simulation result of proposed braking system for 0.3 duty cycle.

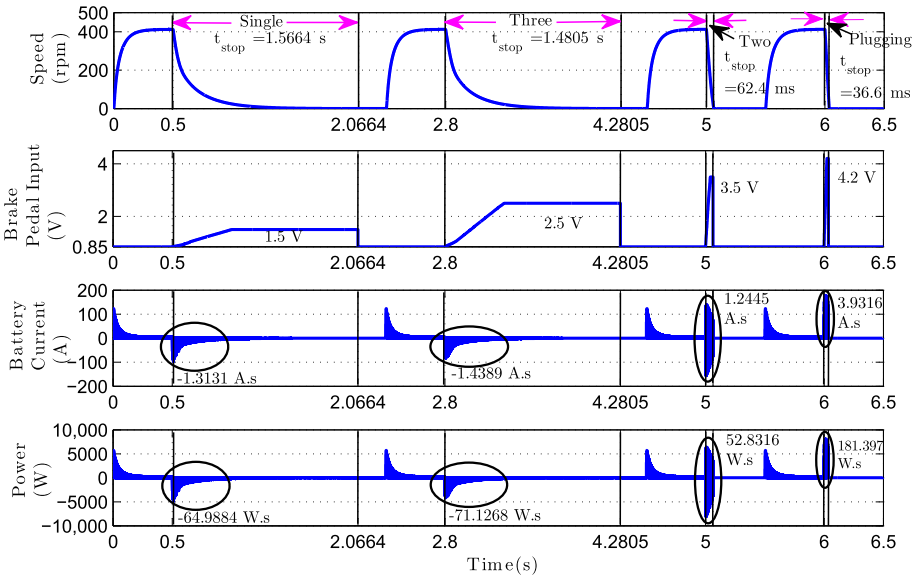

Fig. 12. Simulation result of proposed braking system for 0.7 duty cycle.

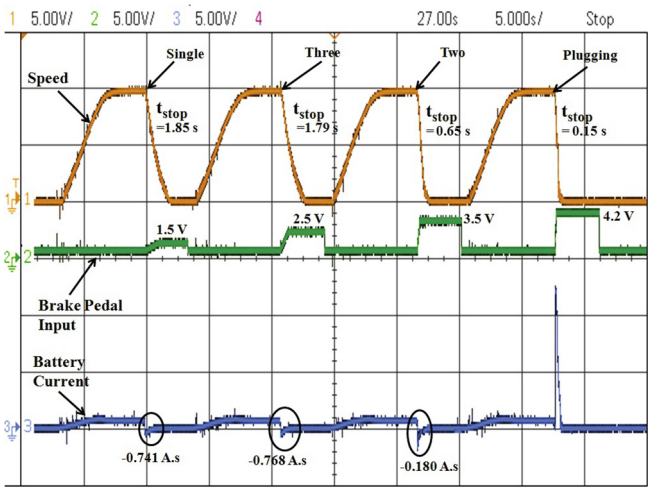

Fig. 13. Experimental result of proposed braking system for 0.3 duty cycle.

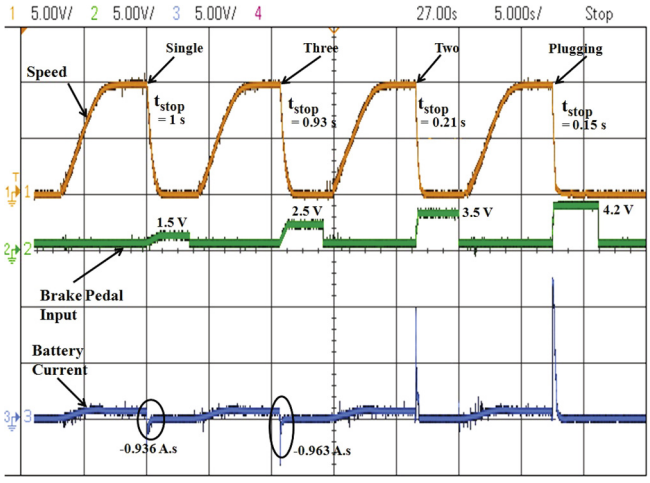

Fig. 14. Experimental result of proposed braking system for 0.7 duty cycle.

is again accelerated to run at steady speed. The brake pedal is depressed again to some more level to activate three switch method. The procedure is repeated for two switch and plugging and the stopping time and energy recovery for each method are measured from the graph. From the results obtained as shown in Figs. 11–14, it can be clearly seen that each braking method is perfectly activated based on the brake pedal input and it is validated that the proposed braking strategy is working effectively with the brake pedal depression.

Figs. 11 and 12 show the simulation results of the proposed braking system for the duty cycle of 0.3 and 0.7. For the duty cycle of 0.3, it can be noted from Fig. 11 that, the stopping time decreases in the order of single switch, three switch, two switch and plugging. With the duty cycle increase (i.e 0.7), as shown in Fig. 12, the stopping of each braking method is further reduced and the same pattern is followed as observed in the performance evaluation. The energy recovered by three switch is higher than single switch in both the duty cycle. In two switch method, the proportion of energy recovered by the battery is more for 0.3 duty cycle and the proportion of energy recovered is less for 0.7 duty cycle. In plugging, the amount of energy consumed is same and finally, it can be observed that all the results are matching with the pattern obtained in performance evaluation.

Similarly, experiments are conducted for the same duty cycle as carried out in the simulation. Figs. 13 and 14 show the experimental results of the proposed braking system for 0.3 and 0.7 duty cycle. The stopping time of each braking method decreases with the same pattern against the increase in the duty cycle as observed in the simulation results. Moreover, the pattern of energy recovery of each braking method is also identical with the simulation results. However, even the pattern of the result is same, it can be noted that there is a mismatch between the simulation and experimental results in terms of stopping time and energy values. This is due to the difference between the theoretical model used in the simulation and the actual model of the experimental setup. The model mismatch is due to the time-varying friction of the motor considered for the experimental study.

5. Conclusion

A novel electric braking strategy based on the brake pedal depression is proposed in this paper. Various existing braking

methods such as single, two, three switch topologies and plugging are combined to achieve this new braking strategy. Two important parameters namely stopping time and energy regeneration are considered to arrive at this proposed scheme. As a first step, their performances are studied using both numerical simulation and experiments. It is concluded that the regeneration is better for single, three switch method and stopping time is better for two switch and plugging. Based on these results, the new braking strategy is designed to switch among single, two, three switch topologies and plugging using brake pedal depression. The proposed strategy is able to stop the vehicle at any speed with possible energy regeneration. Simulation and experimental results are presented to show the effectiveness of the proposed method.

References

[1] M. Ehsani, Y. Gao, A. Emadi, Modern Electric, Hybrid Electric, and Fuel Cell Vehicles: Fundamentals, Theory, and Design, CRC Press, 2009.

[2] M.S. Kumar, S.T. Revankar, Development scheme and key technology of an electric vehicle: an overview, Renew. Sustain. Energy Rev. 70 (2017) 1266–1285.

[3] C.-L. Jeong, J. Hur, A novel proposal to improve reliability of spoke-type BLDC motor using ferrite permanent magnet, IEEE Trans. Ind. Appl. 52 (5) (2016) 3814–3821.

[4] Y.-H. Hung, C.-H. Wu, A combined optimal sizing and energy management approach for hybrid in-wheel motors of evs, Appl. Energy 139 (2015) 260–271.

[5] L. Li, X. Li, X. Wang, J. Song, K. He, C. Li, Analysis of downshift's improvement to energy efficiency of an electric vehicle during regenerative braking, Appl. Energy 176 (2016) 125–137.

[6] L. Zhe, Z. Ling, R. Yue, Y. Wei, L. Yinong, G. Feng, L. Yusheng, X. Zhoubin, A control strategy of regenerative braking system for intelligent vehicle, IET International Conference on Intelligent and Connected Vehicles (ICV 2016), IET, 2016.

[7] C. Pan, L. Chen, L. Chen, H. Jiang, Z. Li, S. Wang, Research on motor rotational speed measurement in regenerative braking system of electric vehicle, Mech. Syst. Signal Process. 66–67 (2016) 829–839.

[8] T. Kim, Regenerative braking control of a light fuel cell hybrid electric vehicle, Electr. Power Components Syst. 39 (5) (2011) 446–460.

[9] O.C. Onar, A. Khaligh, A novel integrated magnetic structure based dc/dc converter for hybrid battery/ultracapacitor energy storage systems, IEEE Trans. Smart Grid 3 (1) (2012) 296–307.

[10] O. Hegazy, J. Van Mierlo, P. Lataire, Analysis, modeling, and implementation of a multidevice interleaved dc/dc converter for fuel cell hybrid electric vehicles, IEEE Trans. Power Electron. 27 (11) (2012) 4445–4458.

[11] X. Zhang, Sensorless induction motor drive using indirect vector controller and sliding-mode observer for electric vehicles, IEEE Trans. Veh. Technol. 62 (7) (2013) 3010–3018.

[12] A. Khaligh, Z. Li, Battery, ultracapacitor, fuel cell, and hybrid energy storage systems for electric, hybrid electric, fuel cell, and plug-in hybrid electric vehicles: State of the art, IEEE Trans. Vehicular Technol. 59 (6) (2010) 2806–2814.

[13] Z. Song, J. Li, X. Han, L. Xu, L. Lu, M. Ouyang, H. Hofmann, Multi-objective optimization of a semi-active battery/supercapacitor energy storage system for electric vehicles, Appl. Energy 135 (2014) 212–224.

[14] J. Armenta, C. Núñez, N. Visairo, I. Lázaro, An advanced energy management system for controlling the ultracapacitor discharge and improving the electric vehicle range, J. Power Sources 284 (2015) 452–458.

[15] F. Naseri, E. Farjah, T. Ghanbari, An efficient regenerative braking system based on battery/supercapacitor for electric, hybrid, and plug-in hybrid electric vehicles with BLDC motor, IEEE Trans. Veh. Technol. 66 (5) (2017) 3724–3738.

[16] Y.-P. Yang, J.-J. Liu, T.-J. Wang, K.-C. Kuo, P.-E. Hsu, An electric gearshift with ultracapacitors for the power train of an electric vehicle with a directly driven wheel motor, IEEE Trans. Veh. Technol. 56 (5) (2007) 2421–2431.

[17] Y.-P. Yang, J.-J. Liu, T.-H. Hu, An energy management system for a directly-driven electric scooter, Energy Conversion Manage. 52 (1) (2011) 621–629.

[18] C.-H. Chen, W.-C. Chi, M.-Y. Cheng, Regenerative braking control for light electric vehicles, 2011 IEEE Ninth International Conference on Power Electronics and Drive Systems (PEDS), IEEE, 2011, pp. 631–636.

[19] W.-C. Chi, M.-Y. Cheng, C.-H. Chen, Position-sensorless method for electric braking commutation of brushless dc machines, IET Electr. Power Appl. 7 (9) (2013) 701–713.

[20] X. Nian, F. Peng, H. Zhang, Regenerative braking system of electric vehicle driven by brushless dc motor, IEEE Trans. Ind. Electron. 61 (10) (2014) 5798–5808.

[21] M.-J. Yang, H.-L. Jhou, B.-Y. Ma, K.-K. Shyu, A cost-effective method of electric brake with energy regeneration for electric vehicles, IEEE Trans. Ind. Electron. 56 (6) (2009) 2203–2212.

[22] Y. Wang, X. Zhang, X. Yuan, G. Liu, Position-sensorless hybrid sliding-mode control of electric vehicles with brushless dc motor, IEEE Trans. Vehicular Technol. 60 (2) (2011) 421–432.

[23] G. Xu, K. Xu, C. Zheng, X. Zhang, T. Zahid, Fully electrified regenerative braking control for deep energy recovery and maintaining safety of electric vehicles, IEEE Trans. Veh. Technol. 65 (3) (2016) 1186–1198.

[24] M. Paredes, J.A. Pomilio, A.A. Santos, Combined regenerative and mechanical braking in electric vehicle, 2013 Brazilian Power Electronics Conference, IEEE, 2013, pp. 935–941.

[25] J. Ko, S. Ko, H. Son, B. Yoo, J. Cheon, H. Kim, Development of brake system and regenerative braking cooperative control algorithm for automatic-transmission-based hybrid electric vehicles, IEEE Trans. Veh. Technol. 64 (2) (2015) 431–440.

[26] M. Rakesh, P. Narasimham, Different braking techniques employed to a brushless dc motor drive used in locomotives, Int. Electr. Eng. J 3 (2) (2012) 784–790.

[27] Ormec, Dynamic braking using external resistors, [Accessed: 10 Sep 2017] (1997). http://www.ormec.com/LinkClick.aspx?fileticket=r4D8nVsbJbY=.